Original Article

MOLECULAR METABOLISM

Protective roles of adiponectin and molecular signatures of HNF4α and PPARα as downstream targets of adiponectin in pancreatic β cells

Toshiharu Onodera [1,6], Dae-Seok Kim [1,6], Risheng Ye [1], May-Yun Wang [1], Shiuhwei Chen [1], Bianca C. Field [1], Leon Straub [1], Xue-Nan Sun [1], Chao Li [1], Charlotte Lee [2], Megan Paredes [1], Clair Crewe [1,3,4], Shangang Zhao [1,5], Christine M. Kusminski [1], Ruth Gordillo [1], Philipp E. Scherer [1,*]

ABSTRACT

The disease progression of the metabolic syndrome is associated with prolonged hyperlipidemia and insulin resistance, eventually giving rise to impaired insulin secretion, often concomitant with hypoadiponectinemia. As an adipose tissue derived hormone, adiponectin is beneficial for insulin secretion and β cell health and differentiation. However, the down-stream pathway of adiponectin in the pancreatic islets has not been studied extensively. Here, along with the overall reduction of endocrine pancreatic function in islets from adiponectin KO mice, we examine PPARα and HNF4α as additional down-regulated transcription factors during a prolonged metabolic challenge. To elucidate the function of β cell-specific PPARα and HNF4α expression, we developed doxycycline inducible pancreatic β cell-specific PPARα (β-PPARα) and HNF4α (β-HNF4α) overexpression mice. β-PPARα mice exhibited improved protection from lipotoxicity, but elevated β-oxidative damage in the islets, and also displayed lowered phospholipid levels and impaired glucose-stimulated insulin secretion. β-HNF4α mice showed a more severe phenotype when compared to β-PPARα mice, characterized by lower body weight, small islet mass and impaired insulin secretion. RNA-sequencing of the islets of these models highlights overlapping yet unique roles of β-PPARα and β-HNF4α. Given that β-HNF4α potently induces PPARα expression, we define a novel adiponectin-HNF4α-PPARα cascade. We further analyzed downstream genes consistently regulated by this axis. Among them, the islet amyloid polypeptide (IAPP) gene is an important target and accumulates in adiponectin KO mice. We propose a new mechanism of IAPP aggregation in type 2 diabetes through reduced adiponectin action.

Keywords Adiponectin; PPARα; HNF4α; β cell

Significance

Adiponectin is a key determinant of pancreatic islet health. We have previously shown that adiponectin is a potent mediator of β cell regeneration after an apoptotic insult. We further expand these observations by showing that adiponectin null mice display reduced expression of critical hormones from α, β, γ and δ cells with reduced HNF4α and PPARα levels. We define a novel adiponectin-HNF4α-PPARα cascade by generating inducible β cell-specific overexpression models for PPARα and HNF4α. While these factors are anti-lipotoxic, they deteriorated the phospholipid levels. Islet amyloid polypeptide (IAPP) is increased by lack of adiponectin, hence exerting a negative impact on insulin release.

Our results shed light on the intracellular signaling cascades induced by adiponectin and further highlight adiponectin as a major player maintaining normal islet function.

[1]Touchstone Diabetes Center, The University of Texas Southwestern Medical Center, Dallas, United States [2]Center for Hypothalamic Research, University of Texas Southwestern Medical Center, Dallas, TX, USA

[3] Current address: Department of Cell Biology and Physiology, Washington University School of Medicine, St. Louis, MO, USA.
[4] Current address: Department of Internal Medicine, Division of Endocrinology, Metabolism and Lipid Research, Washington University School of Medicine, St. Louis, MO, USA.
[5] Current address: Sam and Ann Barshop Institute for Longevity and Aging Studies, Division of Endocrinology, Department of Medicine, University of Texas Health Science Center at San Antonio, San Antonio, TX, 78229, USA.
[6] Equal Contribution.

*Corresponding author.Touchstone Diabetes Center, Department of Internal Medicine, The University of Texas Southwestern Medical Center, Dallas, United States. Tel.: +214 648 8715; fax: +214 648 8720. E-mail: Philipp.Scherer@utsouthwestern.edu (P.E. Scherer).

Received July 10, 2023 • Revision received September 29, 2023 • Accepted October 3, 2023 • Available online 6 October 2023

https://doi.org/10.1016/j.molmet.2023.101821

1. INTRODUCTION

Typically in type 2 diabetes, the accumulation of risk factors, such as obesity, hyperlipidemia and hyperglycemia progressively impact and impair pancreatic β cell function [1]. Excessive circulating lipid and glucose levels induce glucose desensitization, β cell exhaustion and eventually culminates in the β cell death [2] through the induction of ER stress, inflammation and apoptosis [3–5].

Adiponectin is a secreted protein from adipocytes and critically important for the regulation of lipid metabolism, best known for the reduction of lipotoxic species such as ceramide levels. Serum adiponectin levels inversely correlate with proinsulin levels. Although adiponectin is lowered by obesity, adiponectin has been reported to be an independent determinant of the proinsulin to insulin ratio, regardless of adiposity [6]. Mechanistically, adiponectin enhances insulin secretion [7,8] and the regeneration of pancreatic β cells by preserving the β cells from cell death [9,10]. This effect is thought to be maintained through adiponectin receptors (AdipoRs), since AdipoR agonists prevents the palmitate-mediated β cell death by decreasing ceramide levels [11,12].

We have previously reported that overexpression of adiponectin enhances lipid metabolism and β cell regeneration along with the activation of *Peroxisome proliferator-activated receptor alpha* (*PPARα*) and HNF4α pathway in pancreatic β cells [10]. Since PPARα is an AdipoR2 downstream target, PPARα may play a vital role in preventing β cell death or supporting proliferation of β cells through the AdipoR2 axis [13].

The aim of our study is to elucidate the mechanisms of insulin secretion and lipid metabolism, especially aspects regulated by adiponectin. We found that PPARα and HNF4α are strongly affected by adiponectin deficiency. We assessed the *in vivo* effects of PPARα and HNF4α on islet function by utilizing doxycycline-inducible pancreatic β cell-specific PPARα and HNF4α overexpression models.

2. RESEARCH DESIGN AND METHODS

2.1. Mice

The *TRE-Ppara* transgene construct was generated by subcloning a 1,407-bp mouse *Ppara* coding DNA sequence into a plasmid harboring an upstream 0.4-kb *TRE* promoter. The *TRE-Hnf4a* transgene construct was generated by subcloning 1359-bp mouse *Hnf4a* coding DNA sequence into a plasmid harboring an upstream 0.4-kb *TRE* promoter. *TRE-Ppara* and *TRE-Hnf4a* transgenic founder mice were generated by the University of Texas Southwestern Medical Center (UTSW) Transgenic Core. The transgenic strains *MIP-rtTA* [14] was previously generated and characterized by our laboratory. All mouse strains were maintained on a pure C57/BL6 genetic background. Mice were housed on a 12-hour dark/light cycle, with *ad libitum* access to water and diet. Diets used in this study include regular chow diet (LabDiet #5058), doxycycline chow diet (600 mg/kg, Bio-Serv #S7123), high-fat diet (HFD, 60 % calorie from fat, Bio-Serv #S1850), and doxycycline HFD (Dox-HFD, 600 mg/kg, 60 % calorie from fat, Bio-Serv #S5867). All protocols for mouse use and euthanasia were reviewed and approved by the Institutional Animal Care and Use Committee of the University of Texas Southwestern Medical Center, Animal Protocol number 2015-101207G.

2.2. Genotyping PCR

Approximately 2 mm of mouse tail tip was incubated in 80 μL 50 mM NaOH at 95 °C for 1.5 h. 8 μL 1M Tris–HCl (pH 8.0) was added for neutralization. After vortexing and a short spin down, 1 μL of supernatant was used as PCR template. Primer pairs for genotyping PCR are listed in Table S1. The PCR program was: 95 °C for 5 min, followed by 35 cycles of 95 °C for 15 s, 62 °C for 30 s, and 72 °C for 30 s, ended with 72 °C for 3 min.

2.2.1. qPCR

Total RNA was extracted with a RNeasy Mini kit (Qiagen #74106) or Trizol (Invitrogen #15596018). cDNA was synthesized with iScript cDNA Synthesis Kit (Bio-Rad #170-8891). Quantitative real-time PCR (qPCR) was performed with the Powerup SYBR Green PCR master mix (Applied Biosystems # A25742) on Quantistudio 6 Flex Real-Time PCR System (Applied Biosystems # 4485694). Primer sequences for qPCR are listed in Table S2.

2.2.2. Systemic tests

For oral glucose tolerance test (OGTT), mice were fasted for 4–6 h and subjected to an oral gavage of dextrose (2.5 mg/g body weight). Tail blood was collected at 0, 15, 30, 60, and 120 min and prepared for serum then assayed for glucose and insulin. Blood glucose and insulin were measured using Contour blood glucose monitor (9545C, Bayer) or an oxidase-peroxidase assay (Sigma P7119) and insulin ELISA (Crystal Chem, Elk Grove village, IL, USA, #90080). Arginine tolerance test (ATT) was performed by intraperitoneal injection of arginine (1 mg/g body weight) after overnight fasting. Blood samples were collected at 0, 5,10 and 15 min.

2.2.3. Immunohistochemistry

Mice were euthanized by cervical dislocation following isoflurane anesthesia. Tissues were immediately collected and fixed in 10 % buffered formalin for 24 h. Afterwards, tissues were rinsed with 50 % ethanol and embedded in paraffin blocks and sliced into 5 μm sections. H&E staining was performed according to the manufacturer's instructions (#ab245880, Abcam).

2.2.4. Immunofluorescence

Pancreas paraffin sections were de-paraffinized and subjected to antigen retrieval (Dako) and blocking in PBS with Aquablock buffer and goat serum. Primary antibodies used for immunofluorescence are as follows: Insulin (A0564, Dako), glucagon (#ab92517, Abcam) and PPY (#ab272732, Abcam), Iapp (#ab254259, Abcam). Secondary antibodies, alexa Flour 594- and Alexa Flour 488- labeled antibodies (ThermoFisher) were used. Slides were imaged using an inverted Zeiss LSM 780 confocal microscope and analyzed by FIJI/ImageJ.

2.2.5. Islet isolation and GSIS assay

Islet isolation was performed as described [9]. Islets were hand-picked under a dissection microscope and moved to new dishes containing HBSS buffer until free of exocrine pancreas. Tissues were immediately snap frozen in liquid nitrogen followed by storage at −80 °C for qPCR/Western blot analysis or transferred to culture medium for in vitro insulin secretion assays. GSIS assays were conducted as described previously [9]. Briefly, 10-15 islets per sample were equilibrated in 1 mL secretion assay buffer (SAB) with 3 mM glucose for 1 h and then transferred to 1 mL SAB with 3 mM glucose, the low glucose condition. After 1 h incubation, islets were transferred to 1 mL SAB with 16 mM glucose, the high glucose condition. Insulin concentrations in the SAB under both low and high glucose condition were measured for each sample, which were then normalized to the total insulin content of the islets of the sample. Insulin concentrations were measured with an insulin assay kit (ALPCO).

2.2.6. GSIS on perfused pancreata

Perfusions were performed as described [15]. In brief, mouse pancreata were perfused with buffers containing either 5 mM glucose, 20 mM glucose, 2.8 mM glucose and 10 mM Arginine. All buffers before reaching the celiac artery were maintained at 37 °C. Perfusates were then collected at 1-minute intervals for 25 min. Insulin and glucagon levels were measured in perfusates using an insulin assay kit and glucagon assay kit (Cisbio US Inc.).

2.2.7. RNA-seq

RNA-sequence was performed by Novogene (Sacramento, CA, USA) by utilizing isolated RNA from the control kidney and adiponectin overexpressed kidney. After the QC procedures, mRNA from eukaryotic organisms is enriched from total RNA using oligo(dT) beads. For prokaryotic samples, rRNA is removed using a specialized kit that leaves the mRNA. The mRNA from either eukaryotic or prokaryotic sources was then fragmented randomly in fragmentation buffer, followed by cDNA synthesis using random hexamers and reverse transcriptase. After first-strand synthesis, a custom second-strand synthesis buffer (Illumina) is added, with dNTPs, RNase H and *Escherichia coli* polymerase I to generate the second strand by nick-translation and AMPure XP beads are used to purify the cDNA. The final cDNA library is ready after a round of purification, terminal repair, A-tailing, ligation of sequencing adapters, size selection and PCR enrichment. Library concentration was first quantified using a Qubit 2.0 fluorometer (Life Technologies), and then diluted to 1 ng/μl before checking insert size on an Agilent 2100 and quantifying to greater accuracy by quantitative PCR (Q-PCR) (library activity >2 nM). Libraries are fed into Novaseq6000 machines according to activity and expected data volume.

2.2.8. Bioinformatic analysis

Differential expression of genes between Control and AKO were analyzed by using genes with an fpkm of ≥ 0 in all samples. To generate a heatmap, significantly changed protein coding genes were extracted from the original fpkm expression data. Hierarchical clustering was performed after normalization based on Z-score by Morpheus (https://software.broadinstitute.org/morpheus/). The scatter plot was generated by GraphPad Prism (GraphPad, San Diego, Calif., USA). KEGG pathway analysis was performed by Novogene (Sacramento, CA, USA). PPARα and HNF4α target genes were searched by ChIP-Atlas (http://chip-atlas.org/target_genes). Enrichment of significantly changed genes in adiponectin KO islets were analyzed by utilizing genes with an fpkm of ≥ 0 in all samples.

2.2.9. Sphingolipid and phospholipid isolation from tissues

Pancreatic islets preparations (50 islets) were lysed in 500 μL of cold PBS using a sonic probe tissue disruptor at 30 % power (10 cycles of 5 s sonication with 5 s pause). Lysates were prepared one by one while kept in ice bath and immediately quenched in organic solvent. 50 μL of the aqueous lysate was set aside and reserved for BCA (Pierce™ BCA Protein Assay Kit Catalog# 23225). Tissue lysates Sphingolipids. 200 μL of lysate were added to 1.3 mL of cold and quenched with 2.0 mL of organic extraction solvent (isopropanol: ethyl acetate, 15:85; v/v). Immediately afterwards, 20 μL of organic internal standard solution was added (Ceramide/Sphingoid Internal Standard Mixture II diluted 1:10 in ethanol methanol combined with a mixture of C16 Ceramide-d7 (d18:1-d7/16:0), C18 Ceramide-d7 (d18:1-d7/18:0), C24 Ceramide-d7 (d18:1-d7/24:0), and C24:1 Ceramide-d7 (d18:1-d7/24:1(15Z)) at a concentration of 2.4 μM, Avanti Polar Lipids, Alabaster, AL). Two-phase liquid—liquid extraction was performed. The upper phase was transferred to a new clean tube and the lower aqueous phase containing the protein pellet was re-extracted with additional 2.0 mL of organic extraction solvent. The organic phases were combined and dried under nitrogen stream at 40 °C. For analysis of ceramides and sphingoid base species the dried residues were reconstituted in 200 μL of methanol. Sphingomyelins required a sample dilution of 1:50 in methanol prior to analysis.

Phospholipids. 200 μL of the pancreatic preparation aqueous lysate was quenched with 2.0 mL of Folch's solution. Immediately afterwards, 20 μL of SPLASH LIPIDOMIX Mass Spec Internal Standard, diluted 1:10 in MeOH, was added (Avanti Polar Lipids, Alabaster, AL). The mixture was vortex mixed and centrifuged. One-phase extraction was performed. The Supernatant was transferred to a new clean tube and the protein pellet was re-extracted with 2.0 mL of Folch's solution. Organic extracts were dried under nitrogen stream with no heat. Samples were reconstituted in 250 μL MeOH/CH2Cl2 1:1 (v/v).

2.2.10. Mass spectrometry lipids measurement and quantitation

Sphingolipids. 5 μL of reconstituted samples was injected into an LC/MS/MS system for the analysis of ceramides and sphingoid bases, 1 μL injection was required for the analysis of sphingomyelins. The system consisted of a Shimadzu LCMS-8050 triple quadrupole mass spectrometer with the dual ion source operating in electrospray positive ionization mode. The mass spectrometer is coupled to a Shimadzu Nexera X2 UHPLC system equipped with three solvent delivery modules LC-30AD, three degassing units DGU-20A5R, an auto-sampler SIL-30ACMP and a column oven CTO-20AC operating at 40 °C (Shimadzu Scientific Instruments, Columbia, MD). Six sphingoid bases (d18:1 sphingosine, d18:1 sphingosine-1-phosphate, d18:1 deoxysphingosine, d18:0 sphinganine, d18:0 sphinganine-1-phosphate, d18:0 deoxysphinganine) and seventeen ceramide species and their metabolites (C14:0, C16:0, C16:0 dihydroceramide, C16:0 glucosylceramide, C16:0 lactosylceramide, C16:0 sphingomyelin, C18:0, C18:0 dihydroceramide, C18:0 glucosylceramide, C18:0 sphingomyelin, C18:1, C20:0, C22:0, C22:0 glucosylceramide, C24:0, C24:0 dihydroceramide, C24:0 lactosylceramide, C24:0 sphingomyelin, C24:1, C24:1 dihydroceramide, C24:1 glucosylceramide, C24:1 sphingomyelin). Quantitative analysis of sphingolipids was achieved using selective reaction monitoring scan mode. Lipid separation was achieved by reverse phase LC on a 2.1 (i.d.) x 150 mm Ascentis Express C8, 2.7 micron (Supelco, Bellefonte, PA) column under gradient elution, using three different mobile phases: eluent A consisting of methanol/water/formic acid, 600/400/0.8, v/v/v with 5 mM ammonium formate, eluent B consisting of methanol/formic acid, 1,000/0.8, v/v with 5 mM ammonium formate, and eluent C consisting of CH_3OH/CH_2Cl_2 350/650, v/v. The concentration of each metabolite was determined according to calibration curves using the peak-area ratio of analyte vs. corresponding internal standard. Calibration curves were generated using serial dilutions of each target analyte.

Phosphatidylcholines and phosphatidylethanolamines semiquantitative profiling was performed using the mass spectrometric parameters and separations conditions described in the Shimadzu LC-MS/MS MRM Library for Phospholipid Profiling on a Nexera X2 UHPLC coupled to an LCMS-8060 (Shimadzu Scientific Instruments).

LabSolutions V 5.82 and LabSolutions Insight V 2.0 program packages were used for mass spectrometry data processing (Shimadzu Scientific Instruments) [16].

2.3. Statistics

Unpaired two-tailed student's t-tests were applied for all pairwise comparisons. For the tolerance tests, p-values were determined by

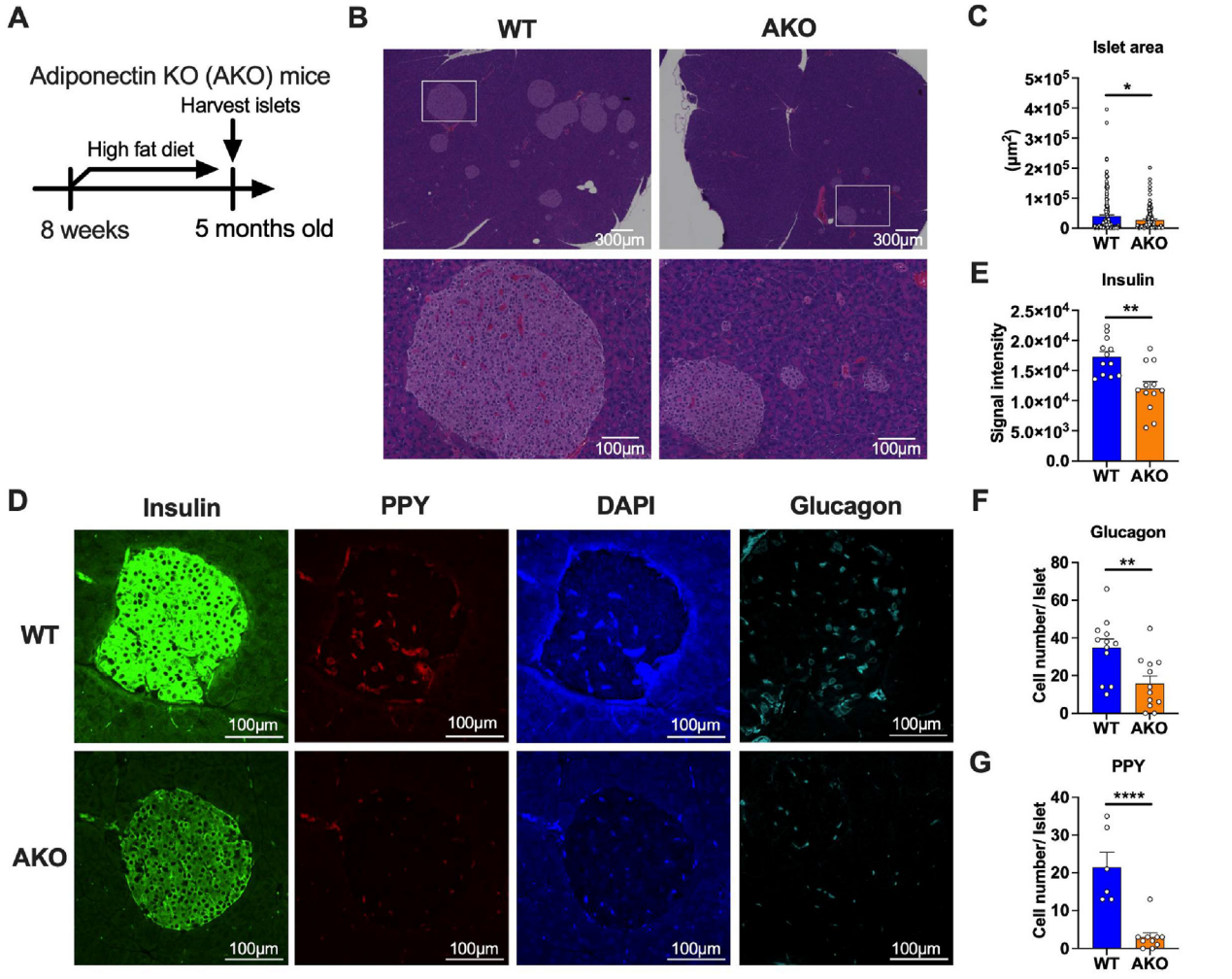

Figure 1: *Adiponectin KO islets show decreased islet size, reduced number of glucagon$^+$ cells and pancreatic polypeptide$^+$ cells.* **(A)** Adiponectin KO mice were fed with HFD from 8 weeks to 5 months old followed by harvesting pancreata and performing histology. **(B)** Representative H&E staining image of islets of adiponectin KO mice under HFD. The scale bar (white line) indicates 300 μm (upper panel) and 100 μm (lower panel), respectively. **(C)** Quantitation of islet areas (μm^2). Dots represent areas of individual islets. n = 2, 5 fields were captured in each slide. **(D)** Immunofluorescence staining of adiponectin KO islets. Insulin (green), PPY (red), DAPI (blue) and Glucagon (Cyan). Glucagon image is derived from the separate section. Scale bar indicates 100 μm. **(E)** Quantitation of average signal intensity of insulin. Dots represent insulin signal intensity in each individual islet. N = 2, 3-6 fields were captured in each slide. **(F)** Quantitation of the number of glucagon$^+$ cells in each islet. N = 2, 3-6 fields were captured in each slide. **(G)** Quantitation of the number of PPY$^+$ cells in each islet. N = 2, 3-6 fields were captured in each slide. Data are mean ± SEM. $*P < 0.05$, $**P < 0.01$ and $****P < 0.0001$. Unpaired 2-tailed t-tests were utilized for determining the p-values for (**C**), (**E**), (**F**) and (**G**).

two-way ANOVA followed by Sidak's multiple comparison test. Statistical significance was accepted at $P < 0.05$.

3. RESULTS

Adiponectin KO islets show decreased islet size, reduced number of glucagon positive cells and pancreatic polypeptide positive cells with overall reduced levels of insulin, glucagon and pancreatic polypeptide. To investigate the role of adiponectin on the pancreatic islets under metabolically challenging conditions, we subjected the adiponectin KO (AKO) mice to a high fat diet for 3 months and performed a histological and immunohistochemical analysis (Figure 1A). Our histological analysis revealed a significantly decreased area of islets in AKO mice, although the overall structure of the islets was not altered by adiponectin deficiency (Figure 1B,C). Even under normal chow diet conditions that do not induce body weight changes, the total islet area is significantly reduced in AKO mice (Figure S1A, B and C). This data suggests that either the HFD-mediated islet proliferation is impaired or there is less insulin resistance in the adiponectin KO mice. In addition to the reduced size of islets in the adiponectin KO mice, the immunofluorescence intensity of insulin is significantly reduced in adiponectin KO islets (Figure 1D,E). Along with insulin staining, staining of additional hormones, such as glucagon from α cells and pancreatic polypeptide (PP) cells were reduced (Figure 1D,F and G). This data suggest adiponectin deficiency affects not only pancreatic β cells, but other endocrine cells in the islets as well.

3.1. Adiponectin deficiency has a broad impact on islet gene expression, specifically lowering PPARα and HNF4α expression

To explore the *in vivo* function of adiponectin on gene expressions of pancreatic β cells, we exposed adiponectin KO mice to a high fat diet for 3 months and subsequently conducted RNA sequencing (RNA-seq) with the isolated islet RNA. Principal component analysis showed a distinct gene signatures between wildtype (Control) and adiponectin

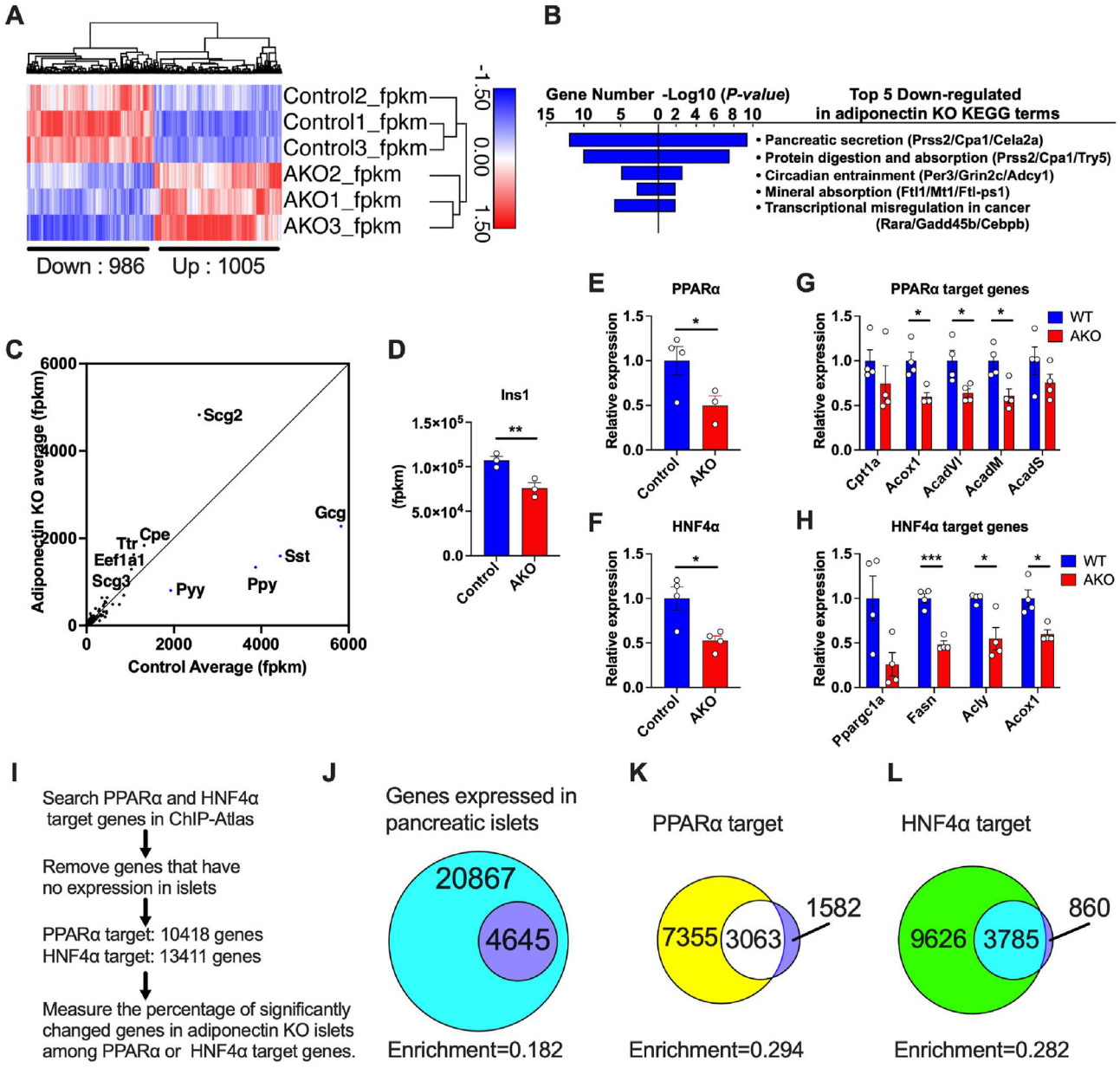

Figure 2: *Adiponectin deficiency lowers endocrine pancreas function related genes, including PPARα and HNF4α expression in the islets.* Adiponectin KO mice were fed with HFD starting at 8 weeks of age for 5 months followed by harvesting pancreatic islets. Total RNA was extracted from the islets and utilized for mRNA-sequencing (RNA-seq). (n = 3) **(A)** Hierarchical clustering of transcriptomes of wild type and adiponectin KO islets. (n = 3) The genes whose adjusted p-value are less than 0.05 among protein coding genes are shown in the heatmap. The number of up-regulated and down-regulated genes are described at the bottom of the heatmap. **(B)** The top 5 down-regulated pathways in adiponectin KO islets by KEGG pathway analysis. (n = 3) **(C)** Scatter plot of the RNA-seq. X-axis; the average of control fpkm, Y-axis; the average of adiponectin KO fpkm. (n = 3) **(D)** Ins1 expression in adiponectin KO islets. (n = 3) **(E)** PPARα expression in the adiponectin KO islets. (n = 3–4) **(F)** HNF4α expression in the adiponectin KO islets. (n = 4) **(G)** mRNA expressions of PPARα target genes. (n = 4) **(H)** mRNA expressions of HNF4α target genes. (n = 4) **(I)** The scheme of the procedure for analyzing the relationship between transcriptional targets and differentially expressed genes in adiponectin KO islets. **(J)** The Venn diagram representing the genes expressed in pancreatic islets (cyan + purple area) and differentially expressed genes in adiponectin KO islets (purple area). The enrichment is the proportion of purple area to whole genes expressed in islets (cyan + purple area). **(K)** The Venn diagram demonstrating the relationship between PPARα target genes (yellow + white area) and differentially expressed genes in adiponectin KO islets (white + purple area). The enrichment is the proportion of white area to PPARα target genes. **(L)** The Venn diagram demonstrating the relationship between HNF4α target genes (green + cyan area) and differentially expressed genes in adiponectin KO islets (cyan + purple area). The enrichment is the proportion of cyan area to HNF4α target genes. Data are presented as mean ± SEM. $*P < 0.05$, $**P < 0.01$ and $***P < 0.001$. Unpaired 2-tailed t-tests were utilized for determining the p-values for **(D)**, **(E)**, **(F)**, **(G)** and **(H)**.

KO (AKO) mice (Fig. S2A). The hierarchical clustering of altered protein-coding genes showed significant changes for 1,005 up-regulated genes and 986 downregulated genes (Figure 2A). Further KEGG pathway analysis revealed that up-regulated genes are enriched in cell cycle and cell division related pathways (Fig. S2B). This enrichment suggests an abnormality high cell proliferation due to adiponectin deficiency. Conversely, the genes down-regulated in adiponectin KO islet were found to be enriched in a number of pathways critical to the islet function (Figure 2B). Particularly, the most down-regulated pathway was the pancreatic secretory pathway, which was specified

by the decreased expression of genes such as *Serine Protease 2* (*Prss2*) and *carboxypeptidase A1* (*Cpa1*). Consistent with this, the RNA-seq scatter plot depicted a strong down-regulation of genes directly involved in endocrine pancreas function, including *glucagon* (*gcg*), *peptide yy* (*pyy*), *somatostatin* (*sst*) and *pancreatic polypeptide* (*ppy*) despite their high expression levels (Figure 2C). Additionally, insulin1 (Ins1) gene expression was significantly reduced by adiponectin deficiency (Figure 2D). These observations indicate that the gene expressions of each representative hormone secreted from α cells, δ cells and PP cells are all impaired by adiponectin deficiency.

We previously identified PPARα and HNF4α as up-regulated transcription factors in regenerated islets upon systemic adiponectin overexpression [10] (Fig. S3A). This previous study focused on islet regeneration after caspase 8 - mediated apoptotic death rather than a dietary high fat diet challenge. We decided to focus on factors that show a diametrically opposed regulation between overexpressing and KO models. To do that, we determined the pathways most affected by the overexpression of adiponectin in the islets. We revisited the data and performed gene ontology (GO) pathway analysis. Six out of the top 10 most highly enriched pathways included lipid metabolism-related pathways (Fig. S3B). Among the lipid metabolism-related transcription factors, PPARα and HNF4α were highly up-regulated by adiponectin overexpression (Fig. S3C). In agreement with this, PPARα and HNF4α target genes were up-regulated as well by the overexpression of adiponectin (Figure 3D and E). This reveals strong symmetry between gain and loss of function adiponectin phenotypes.

To verify the regulation of PPARα and HNF4α by adiponectin, we measured the expressions of PPARα and HNF4α in the adiponectin KO islet by qPCR. In contrast to adiponectin overexpression, we confirmed that the expression levels of PPARα and HNF4α were down-regulated in adiponectin KO settings (Figure 2E,F). This data suggests that, regardless of the regenerative conditions, adiponectin is vital for the maintenance of the expression of PPARα and HNF4α. In light of the lowered expression of these transcription factors, the target genes of PPARα and HNF4α were down-regulated in the adiponectin deficient islets (Figure 2G,H). To expand this concept, we extracted the PPARα and HNF4α target genes from within the ChIP-Atlas (http://chip-atlas.org/target_genes) and removed the genes that are not expressed in islets. We then compared significantly altered genes in the adiponectin KO islets with PPARα targets and HNF4α targets expressed in islets, (Figure 2I). 4,645 genes were significantly changed in adiponectin KO islets among 25,512 genes that are expressed in islets (Figure 2J). 10,418 PPARα target genes included 3,063 genes that were significantly changed in adiponectin KO islets (Figure 2K). 13,411 HNF4α target genes contained 3,785 genes altered in adiponectin KO islets (Figure 2L). Relative enrichment of the altered genes in adiponectin KO islets is increased to more than 50 % when the genes were limited to PPARα or HNF4α targets (Figure 2J,K and L). In other words, 65.9 % and 81.5 % of significantly changed genes in adiponectin KO islets are PPARα and HNF4α targets, respectively (Figure 2K,L).

3.2. Inducible PPARα overexpression in pancreatic β cells impairs insulin secretion

Since we screened PPARα and HNF4α as potential targets of adiponectin in the pancreatic islets, we opted to investigate the direct impact of PPARα on the pancreatic β cells *in vivo*. We generated a novel transgenic mouse line, *TRE-Ppara*, where the transcription of a mouse PPARα-encoding transgene is driven by a tetracycline responsive element (TRE)-containing promoter. The *TRE-Ppara* strain was crossed with the *MIP-rtTA* transgenic strains to enable doxycycline-inducible overexpression of PPARα specifically in insulin-producing pancreatic β-cells (β-PPARα) (Figure 3A). The *TRE-Ppara*-negative littermates of the PPARα-overexpressing mice that have only *MIP-rtTA* were employed as control mice.

β-PPARα mice were fed a high fat diet (HFD) for 4 months followed by a HFD containing 600 mg/kg doxycycline for 2 weeks to induce PPARα expression (Figure 3B). PPARα mRNA expression was induced significantly in the islets of β-PPARα mice (Figure 3C). PPARα protein was also elevated within a physiological range in β-PPARα islets (Figure 3D). Bodyweights were comparable between the two groups before and after the 2 weeks of doxycycline treatment (Figure 3E). To assess systemic glucose metabolism, we performed systemic tolerance test including an oral glucose tolerance test (OGTT) and an arginine tolerance test (Arginine TT). While serum glucose levels during an oral glucose tolerance test (OGTT) were not altered, serum insulin levels were significantly decreased by PPARα overexpression (Figure 3F,G). These metabolic changes are not associated with changes in food intake (Fig. S4A). These data indicate that β-PPARα overexpression leads to improved insulin sensitivity ostensibly by reducing the serum insulin levels without a concomitant negative impact on blood glucose levels. Using one of the insulin sensitivity indices, the Raynaud index, indicates higher insulin sensitivity (Fig. S4B). On the other hand, arginine TTs revealed lower insulin secretion in β-PPARα overexpression (Figure 3H). Insulin TT (ITT) showed a comparable glucose level between control and β-PPARα overexpressing mice (Fig. S4C). These data indicate that systemic insulin sensitivity is not altered, rather only the insulin levels are reduced in β-PPARα overexpressing mice. Caloric restriction and the reduction of the insulin signaling pathway are beneficial for life span [17]. The chronic reduction of insulin levels is likely favorable for health. This is also in further support of the notion that excess insulin leads to insulin resistance. If increases in insulin release can be prevented, sustained sensitivity prevails with lower insulin levels.

Instead of feeding HFD dox 600 mg for just 2 weeks, we checked the impact of 5 months of PPARα overexpression during HFD dox 600 mg feeding (Fig. S5A). The long-term HFD dox 600 mg feeding did not significantly affect the body weight (Fig. S5B). However, in contrast to the acute 2-week exposure, the blood glucose levels during OGTT were elevated in β-PPARα mice (Fig. S5C). The serum insulin levels during the OGTT and arginine tolerance tests were lowered by this chronic β-PPARα overexpression (Figure 5D and E). This suggests that long term suppression of insulin secretion by PPARα culminates in deteriorated glucose levels during OGTT.

To determine the mechanism whereby insulin secretion is impaired by PPARα overexpression in β-cells, we isolated pancreatic islets and cultured them in the presence of 3 mM or 20 mM glucose. Islets from the control mice showed increased insulin secretion in response to 20 mM glucose. On the other hand, islets from PPARα overexpressing mice showed no significant response to 20 mM glucose (Figure 3I). Although GSIS is impaired by PPARα overexpression, the size of the pancreatic islets determined by histology was not altered by PPARα overexpression (Figure 3J,K). However, the signal intensity of insulin and glucagon was significantly and uniformly reduced in the β-PPARα islets. (Figure 3L,M).

3.3. Inducible PPARα overexpression in pancreatic β cells increases fatty acid oxidation and lowers ceramide content

To corroborate the decreased insulin secretion from β-PPARα islets, we perfused the pancreas with multiple different levels of glucose and evaluated insulin secretion *ex vivo*. Perfusion of pancreata from β-PPARα mice with a high concentration of glucose displayed a blunted spike in the insulin secretion as compared to those from control mice

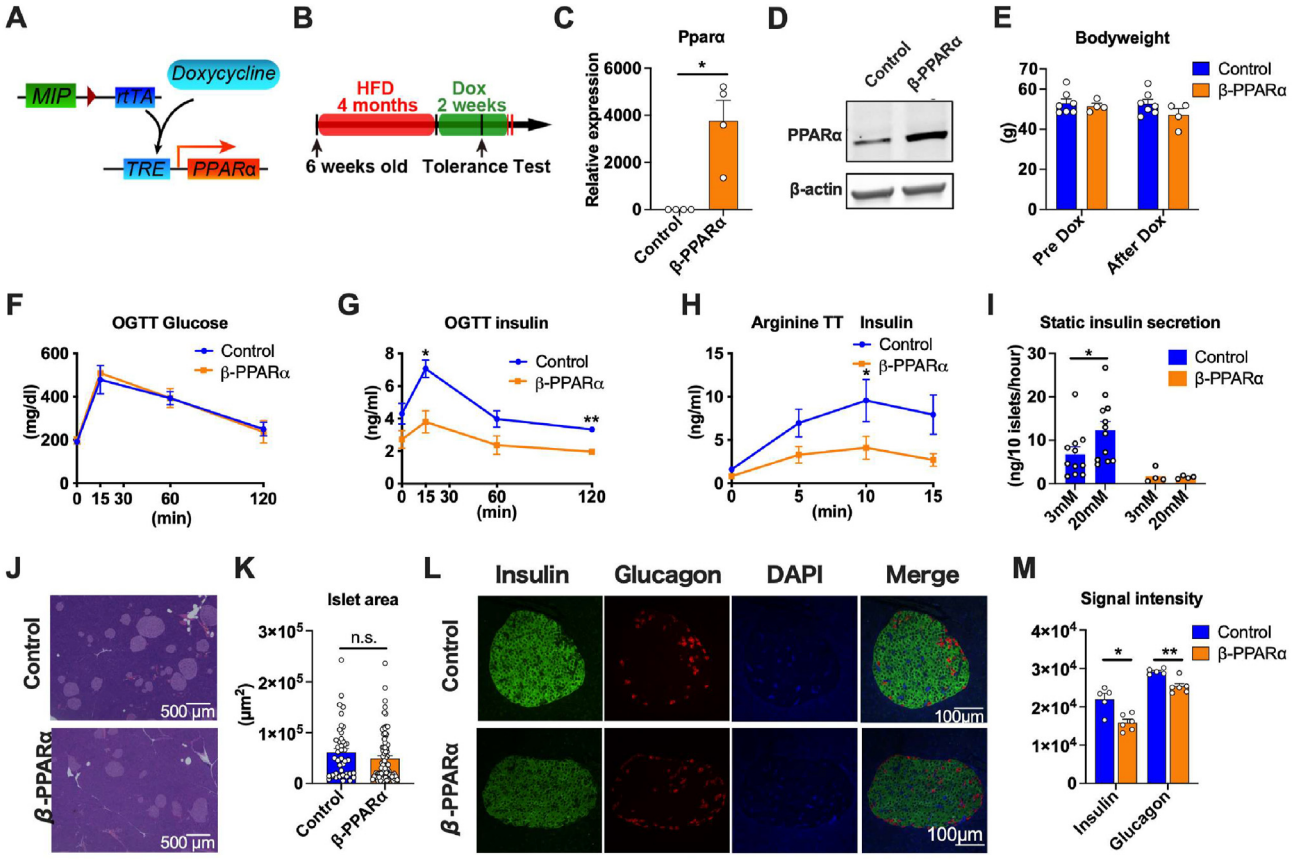

Figure 3: *Inducible PPARα overexpression in pancreatic β cells impairs insulin secretion.* **(A)** The schematic representation of the Doxycycline-inducible PPARα overexpression in pancreatic β cells. rtTA is expressed under the control of mouse insulin promotor (MIP). Doxycycline promotes the binding of rtTA to TRE, that further activates the PPARα expression. Mip-rtTA mice were used as littermate controls. Mip-rtTA/TRE-PPARα were utilized as β cell PPARα overexpression (β- PPARα) mice **(B)** β- PPARα mice were fed with HFD for 4 months from 6 weeks old and switched to doxycycline 600 mg/kg containing HFD (Dox). Systemic tolerance tests were performed 2 weeks after the start of HFD Dox. **(C)** PPARα expression in the β- PPARα. (n = 4–5) **(D)** Representative Western blot image of PPARα in β- PPARα islets. **(E)** The body weight of β- PPARα mice before and after the treatment of HFD Dox. (n = 4–7) **(F)** The blood glucose levels during OGTT (n = 3–5) **(G)** The serum insulin level during OGTT (n = 3–5) **(H)** The serum insulin level during arginine tolerance test (n = 12) **(I)** GSIS of the islets from β-PPARα mice. (n = 4–12) **(J)** Representative H & E staining image of islets of control and β-PPARα mice. The scale bar (black line) indicates 500 μm. **(K)** Quantitation of islet areas. Dots represent individual area of islets. (n = 4) **(L)** Immunofluorescence of the β- PPARα pancreas. Insulin (green), Glucagon (red) and DAPI (blue). Scale bar indicates 100 μm. **(M)** Calculation of signal intensity of insulin and glucagon signal. (n = 5–6) Data are mean ± SEM. $^{*}P < 0.05$ and $^{**}P < 0.01$. 2-way ANOVA with Sidak's multiple comparison test was performed for (**G**) and (**H**). Unpaired 2-tailed t-tests were utilized for determining the p-values for (**C**), (**I**), (**K**) and (**M**).

(Figure 4A). We also evaluated glucagon secretion at 3 levels of glucose concentrations, 5 mM, 20 mM and 2.8 mM. Glucagon secretion was relatively suppressed under high glucose concentrations, but showed no significant changes (Figure 4B). The insulin secretion at each glucose concentration showed a significant decrease at 20 mM glucose concentration by PPARα overexpression (Figure 4C). In contrast, glucagon secretion did not show significant changes (Figure 4D).

We subsequently assessed the mRNA expression associated with β oxidative capacity, insulin secretion and differentiation in pancreatic β cells. The PPARα target genes involved in β oxidation including *Acyl-CoA oxidase1* (*Acox1*) and *Carnitine Palmitoyltransferase 1A* (*Cpt1a*) were significantly up-regulated (Figure 4E). This data confirms the functional overexpression of PPARα and the viability of the islets. In contrast, the expression of transcription factors that are related to β cell differentiation, but not α cell differentiation, were decreased in β-PPARα overexpression. Not only transcription factors, but additional genes that are critical for the β cell function, such as *Glucose transporter2* (*Glut2*), were also down-regulated by PPARα overexpression (Figure 4F). Immunofluorescence did not reveal any macrophage infiltration, neither in controls nor in β-PPARα islets, indicating a negligible contribution of inflammation to this phenotype (Fig. S6A). To assess lipotoxicity levels in the β-PPARα mice, we measured ceramides and their precursors, the dihydro-ceramides. For these ceramide and phospholipid measurements, we utilize β-PPARα mice that were exposed to doxycycline containing HFD for 40 weeks. Consistent with the fact that fatty acid β oxidation is up-regulated in the β-PPARα mice, many of the ceramide species, including ceramide 16:0, showed a significant reduction by β-PPARα overexpression (Figure 4G,H). In addition to the reduction in ceramides, we could also observe a reduction in phospholipids, such as phosphatidylcholine (PC) and phosphatidylethanolamine (PE), integral constituents of cellular membranes. PC species exhibited a reduction across most of the species typically found in this PC group (42:4) and (42:5) (Figure 4I). Total amount of PC levels in β-PPARα islet was significantly decreased as well (Figure 4J). Another major phospholipid, PE, also showed an overall reduction in β-PPARα islets. Particularly, we could observe a striking decrease in PE (42:4) and (42:5), with side chain lengths

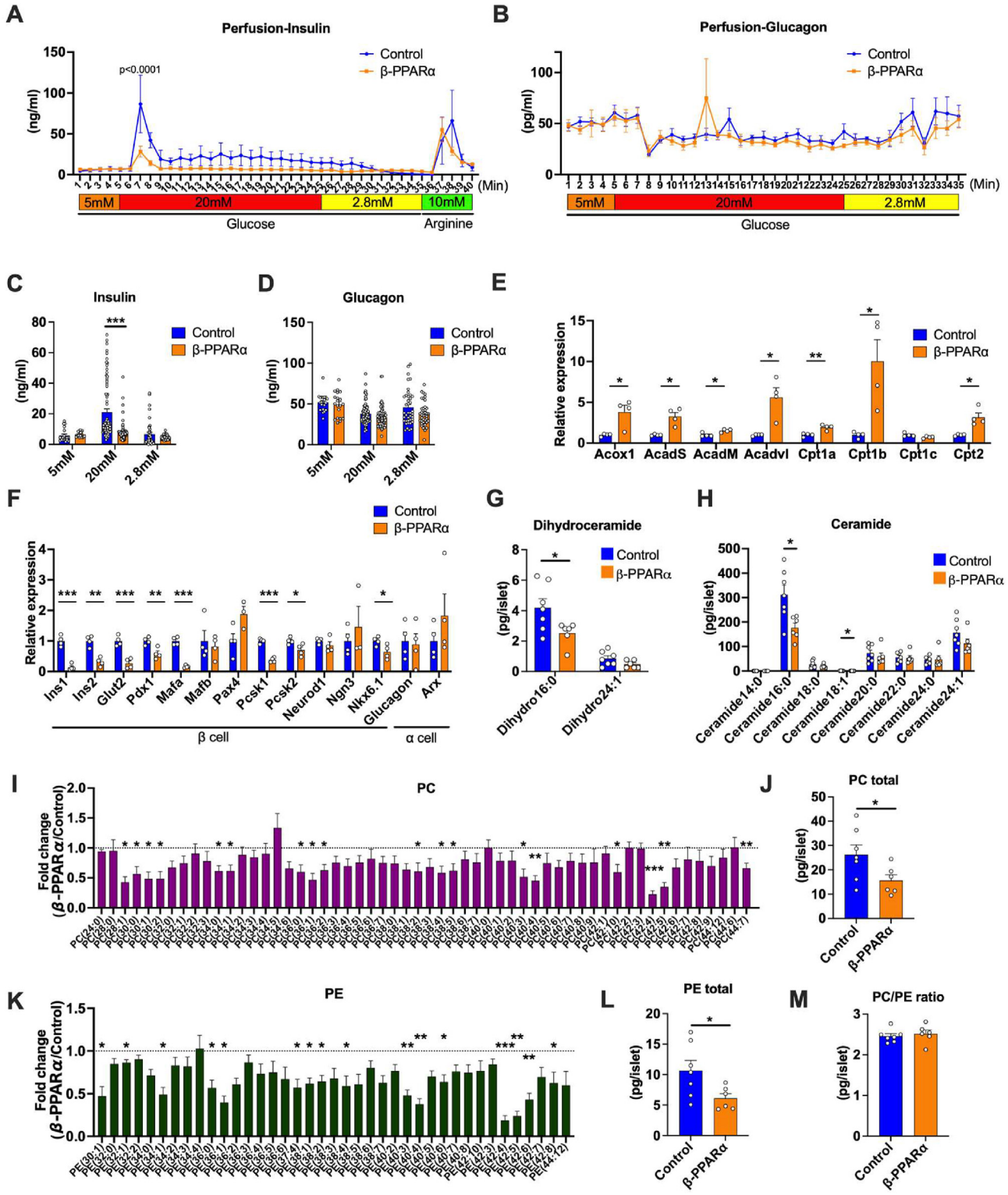

Figure 4: *Inducible PPARα overexpression in pancreatic β cells increases fatty acid oxidation and lowers ceramide content.* **(A)** Insulin secretion rates (ng/ml) during the perfusion of β-PPARα mice pancreas. Glucose concentration was started with 5 mM followed by 20 mM and 2.8 mM (n = 4) **(B)** Glucagon secretion rates (pg/ml) during the perfusion of β-PPARα mice pancreas. (n = 4) (**C**) Average of the insulin secretion rates during the perfusion at each glucose concentration. (**D**) Average of the glucagon secretion rates during the perfusion at each glucose concentration. (**E**) Expressions of genes related to β oxidation in β-PPARα islets. (n = 4) (**F**) Expressions of genes related to β and α cell differentiation and function in β-PPARα islets. (n = 4) (**G**) Dihydroceramide species levels in β-PPARα islets. (n = 6–7) (**H**) Ceramide species levels in β-PPARα islets. (n = 6–7) (**I**) Fold-change of phosphatidylcholine (PC) content in β-PPARα islets over control islets. (n = 6–7) (**J**) Total PC levels in β-PPARα islets. (n = 6–7) (**K**) Fold change of phosphatidylethanolamine (PE) content in β-PPARα islets over control islets. (n = 6–7) (**L**) Total PE levels in β-PPARα islets. (**M**) PC/PE ratio in control and β-PPARα islets. (n = 6–7) Data are mean ± SEM. $*P < 0.05$, $**P < 0.01$ and $***P < 0.001$. 2-way ANOVA with Sidak's multiple comparison test was performed for **(A)** and (**B**). Unpaired 2-tailed t-tests were utilized for determining the p-values for (**C**), (**E**), (**F**), (**G**), (**H**), (**I**), (**J**), (**K**) and (**L**).

similar to what was seen in PC (Figure 4K). Consistent with this, total PE levels were also significantly decreased in β-PPARα islets (Figure 4L). Although lower hepatic PC/PE ratio correlates with NAFLD and NASH phenotypes in humans and rodents [18,19], β-PPARα overexpression had little impact on the actual PC/PE ratio in the pancreatic islets (Figure 4M).

Taken together, this data demonstrates that β-PPARα overexpression results in lowered insulin secretion despite lowered lipotoxicity levels in the islets.

3.4. Inducible HNF4α overexpression in pancreatic β cells impairs the HFD-induced expansion of islets

HNF4α is the second potential target of adiponectin that can facilitate lipid metabolism in the islets. To evaluate the impact of HNF4α on pancreatic β cells, we generated a novel transgenic mouse strain, *TRE-Hnf4α*, where TRE containing promoter accelerates the transcription of HNF4α upon the binding of rtTA. Doxycycline facilitates the binding of rtTA to TRE, and induces the transcription of HNF4α in a doxycycline dependent manner. The *TRE-Hnf4α* strain was crossed with the *MIP-rtTA* transgenic strains that allow us to inducibly overexpress HNF4α specifically in pancreatic β-cells (β-HNF4α) (Figure 5A). We fed β-HNF4α mice a 600 mg/kg doxycycline containing HFD for 3 months followed by systemic tolerance tests (Figure 5B). OGTTs showed significantly higher levels of glucose in β-HNF4α mice (Figure 5E) concomitant with the suppressed serum insulin levels (Figure 5F). Food intake was not altered in β-HNF4α mice (Fig. S6B). These data indicate that hyperglycemia in β-HNF4α mice is caused by a lack of insulin secretion. In accordance with the OGTTs, arginine tolerance tests exhibited significantly lower insulin level in β-HNF4α mice (Figure 5G). Hematoxylin—eosin (HE) staining of pancreas revealed that the area of the islets was significantly decreased in β-HNF4α mice, suggesting that the HFD-induced expansion of islet is impaired in the β-HNF4α mice (Figure 5H,I). Additionally, the arrangement of the nucleus in the islets is distorted by the β-HNF4α overexpression possibly because of the hyperplasia of other cell types in the islets (Figure 5H). In addition to the smaller area of islets, immunofluorescence staining revealed that overall insulin intensity is comparable, but the islets of β-HNF4α mice contain larger insulin negative areas. However, this insulin negative area does not correspond to the glucagon positive cells or macrophages (Figures 5J and S6C).

3.5. Gene signatures of β-PPARα and β-HNF4α islets exhibit the potential pathways of adiponectin actions on pancreatic islets

To determine the molecular cascade of PPARα and HNF4α in pancreatic β-cells, we performed RNA-seq by utilizing the β-PPARα and β-HNF4α islets. β-HNF4α islets showed a high expression of PPARα (Figure 6A), while HNF4α expression was not altered by PPARα overexpression (Figure 6B), indicating that HNF4α is either a direct or indirect upstream mediator of PPARα (Figure 6A,B). Given that adiponectin deficiency reduces the expression of both PPARα and HNF4α, this data suggests a possible axis of adiponectin-HNF4α-PPARα in pancreatic β cells. Principal component analysis (PCA) of RNA-seq data showed the distinct transcriptome signature among controls, β-PPARα and β-HNF4α group (Figure 6C). Although it is well known that PPARα and HNF4α are involved in fatty acid β oxidation, we further clarified the common and distinct roles of PPARα and HNF4α in pancreatic β cells. We determined 1989 and 1508 genes significantly up or resp. down-regulated in β-HNF4α islets, respectively. Additionally, we specified 376 and 431 genes significantly up or resp. down-regulated only in β-PPARα islets, respectively (Figure 6D). Genes regulated by both PPARα and HNF4α were categorized into 4 groups: ***(A)*** the genes *up-regulated by PPARα* but *down-regulated by HNF4α*. ***(B)*** the genes *up-regulated by PPARα* and *HNF4α*. ***(C)*** the genes *down-regulated by PPARα* but *up-regulated by HNF4α*. ***(D)*** the genes *down-regulated by PPARα* and *HNF4α*. Consistent with a previous report in the liver [20], the genes in *Group B* were enriched in the fatty acid oxidation related pathways. The *Group D* genes that were down-regulated in both β-PPARα and β-HNF4α islets were enriched in the insulin secretion pathway, consistent with the phenotypes of β-PPARα and β-HNF4α mice (Figure 6E). To identify the genes that were consistently regulated by the axis of adiponectin-HNF4α- PPARα, we screened the genes that were *up-regulated in adiponectin KO*, *down-regulated in β-HNF4α* and *β-PPARα islets* (Figure 6F) and the genes that were *down-regulated in adiponectin KO*, *up-regulated in β-HNF4α* and *β-PPARα islets* (Figure 6G). Among those genes, we focused on Islet amyloid polypeptide (IAPP) that is also known as amylin. The aggregation of IAPP in the islets represents a pathogenic response seen in type 2 diabetes [21]. We confirmed the up-regulation of IAPP protein in adiponectin KO islets by immunofluorescence (Figure 6H,I). Consistent with this, IAPP protein levels are reduced in β-PPARα and β-HNF4α islets (Figure S7A, B, C and D). Overall, we propose a cascade starting with adiponectin that eventually suppresses IAPP aggregation in islets through HNF4α and PPARα (Figure 6J).

4. DISCUSSION

Here, we found overall endocrine pancreatic function to be dysregulated in islets of systemic adiponectin KO mice. This includes α, β, δ and γ cells. Adiponectin is known to potentiate the insulin secretion in INS1E cells by activating fatty acid oxidation [8] and enhances the regenerative capacity after the induction of caspase-8-mediated β cell death [9]. The genetic loss of the downstream target of AdipoR [22], *Adaptor protein, phosphotyrosine interacting with PH domain and leucine zipper 1* (*APPL1*), disturbs GSIS via impairing mitochondrial biogenesis and function [23], further highlighting the contributions of adiponectin to insulin secretion. Few studies have described the impact of adiponectin on pancreatic endocrine cells other than on β cells. By comparing our results in our previous studies [9] and the current study, we screened PPARα and HNF4α as target transcription factors of adiponectin in the islets. By overexpressing these transcription factors inducibly specifically in pancreatic β cells, we could evaluate the function of PPARα and HNF4α in pancreatic β cells without developmental issues. Since a reduced insulin secretion capacity of β-HNF4α and β-PPARα mice does not fit the phenotype of adiponectin KO mice, we discovered additional potential targets of adiponectin-HNF4α-PPARα pathway, such as IAPP, which we found upon analysis of RNA-Seq data. Suppressing IAPP by adiponectin represents an additional important beneficial role of adiponectin in the pancreatic β cells environment.

We have previously shown that injected recombinant adiponectin accumulates in the pancreatic islets. Adiponectin deficiency further exacerbates islet damage caused by caspase-8-mediated β cell death [24]. Moreover, aged adiponectin KO mice show relatively low insulin levels, despite an elevation of glucose levels during an OGTT [25]. It seems reasonable to speculate that these low serum insulin levels are caused by the direct dysfunction of the pancreatic β cells in these mice.

We also have shown that PPARα was up-regulated by overexpression of adiponectin in regenerating pancreatic islets [10]. It is well established that PPARα mediates fatty acid oxidation, thereby reducing lipotoxicity. We appreciate that lipotoxicity impairs the insulin secretory

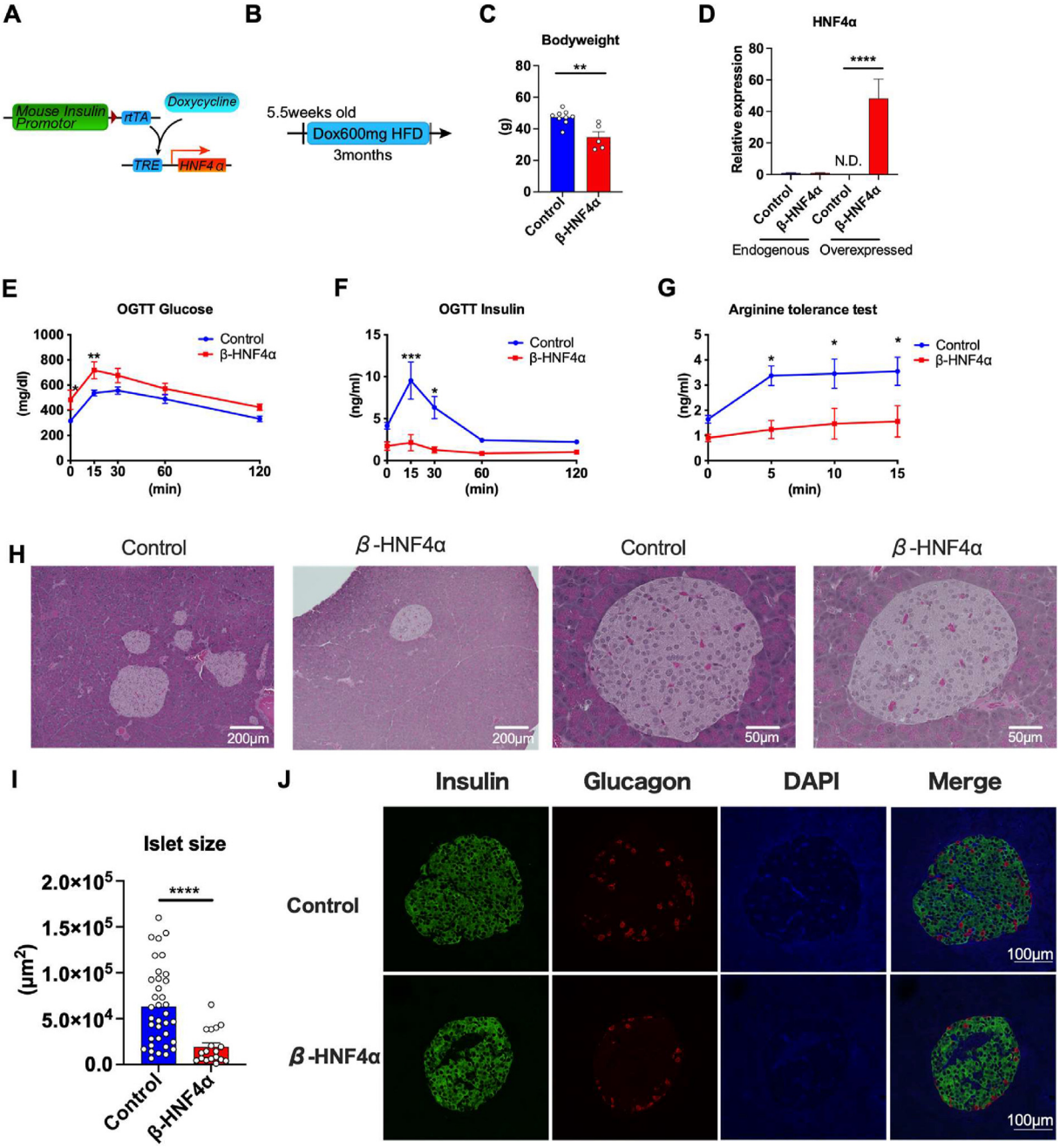

Figure 5: *Inducible HNF4α overexpression in pancreatic β cells impairs the HFD-induced expansion of islets.* **(A)** The schematic representation of the Doxycycline-inducible HNF4α overexpression in pancreatic β cells. rtTA is expressed under the control of mouse insulin promotor (MIP) that enables the pancreatic β cell specific overexpression. Doxycycline promotes the binding of rtTA to TRE, that further activates the PPARα expression. Mip-rtTA mice were used as littermate control. Mip-rtTA/TRE-HNF4α were utilized as β cell HNF4α overexpression (β-HNF4α) mice **(B)** β-HNF4α mice were fed with HFD Dox 600 mg/kg from 5.5 weeks old for 3 months followed by the systemic tolerance test. (**C**) The body weight of β-HNF4α mice after 3 months of HFD Dox feeding. (n = 5–9) (**D**) The expressions of genes of endogenous HNF4α and HNF4α transgene in control and β-HNF4α mice islet. (n = 3) **(E)** Blood glucose level of β-HNF4α mice during OGTT (n = 5–9) **(F)** Serum insulin level of β-HNF4α mice during OGTT (n = 3–6) (**G**) Serum insulin level of β-HNF4α mice during arginine tolerance test (n = 11–6) (**H**) Representative H & E staining image of islets of control and β-HNF4α mice. The scale bar (white line) indicates 200 μm for low-magnification images and 50 μm for high-magnification images. (**I**) Quantitation of islet areas. Dots represent individual area of islets in β-HNF4α pancreata. n = 4 (**J**) Immunofluorescence of the β-HNF4α pancreas. Insulin (green), Glucagon (red) and DAPI (blue). Scale bar indicates 100 μm. Data are mean ± SEM. $*P < 0.05$, $**P < 0.01$, $***P < 0.001$ and $****P < 0.0001$. 2-way ANOVA with Sidak's multiple comparison test was performed for (**E**), (**F**) and (**G**). Unpaired 2-tailed t-tests were utilized for determining the p-values for (**C**), (**D**) and (**I**).

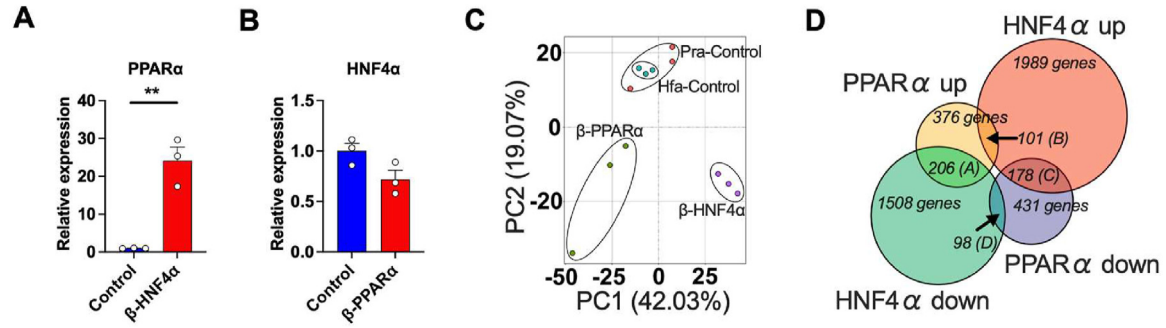

E

Overlapped Group	Top20 gene and major Gene Ontology pathways				
A	Cib3	Acta1	Ccl19	Gpx2	Crlf1
PPARα up, HNF4α down	Etfb	Bok	Arhgdig	Rgs11	Efcab15
206 genes	Lpl	Gsto2	Rnf208	Acaa2	Ppp1r1a
	Rpl21	C2cd4b	Ckb	Tmem88	Rps12
	Ribosomal small subunit assembly (32.92, 4.70E-05)				
	Negative regulation of ubiquitin protein ligase activity (41.7, 2.64E-03)				
B	Gabrd	Slc27a2	Ehhadh	Wnt9a	Aqp7
PPARα up, HNF4α up	Cebpa	Gpd1	St6galnac2	Slc25a10	Sgk2
101 genes	Tst	Ambp	Tmem145	Esrp2	Pth1r
	Acot2	Pde4c	Rcor2	Crat	Egln3
	Very long-chain fatty acid catabolic process (83.32, 9.21E-03)				
	Fatty acid beta-oxidation (38.31, 2.52E-09)				
C	Aldob	Slc26a3	Sult1d1	Selenop	Plekhf1
PPARα down, HNF4α up	Kl	Neb	Cyp4v3	Ptger3	Usp9x
178 genes	Mpp7	Sik2	Ankhd1	Usp34	Il1rap
	Enpp2	Nktr	Atp1b1	Klf15	Vps13c
	Endocrine pancreas development (13.15, 2.38E-02)				
	Acinar cell differentiation (74.15, 1.82E-02)				
D	Dnajb9	Nipsnap2	Cdr2	Hspa5	Slc35b4
PPARα down, HNF4α down	Pdia3	Ap1s2	Tceal9	Tram1	Zdhhc2
98 genes	Sec22b	P2ry1	Atp6v1d	Rab2a	Scg2
	Nkx6-1	Eid1	Fmn2	Atp6ap2	Vamp4
	Protein targeting to ER (20.46, 2.22E-02)				
	Insulin secretion (19.64, 5.27E-03)				

F

Genes: Up in adiponectin KO
Down in β-HNF4α and β-PPARα
Akain1
Atp6ap2
Bet1
Chic1
Cntn1
Efcab1
Eid1
Extl2
Fam210b
Glrb
Gpr158
Gramd3
Hdac9
Iapp
Lrrn1

G

Genes: Down in adiponectin KO
Up in β-HNF4α and β-PPARα
Agpat3
Akap1
Akr7a5
Ankrd13b
Baiap2l2
Cebpa
Dhrs3
Dvl1
Eci1
Gcgr
Gpd1
Gpi1
Gstt2
Kmt5c

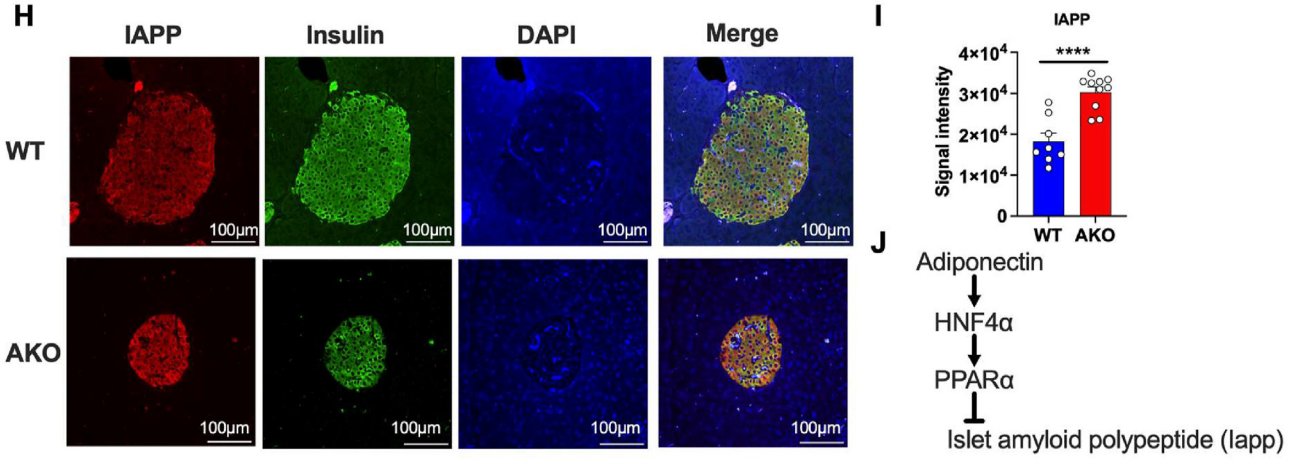

Figure 6: *Gene signatures of β-PPARα and β-HNF4α islets exhibit the potential pathways of adiponectin actions on pancreatic islets.* **(A)** PPARα mRNA expression in β-HNF4α pancreatic islets. (n = 3) **(B)** HNF4α mRNA expression in β-PPARα pancreatic islets. (n = 3) **(C)** Principal component analysis of transcriptome signatures of β-PPARα and β-HNF4α pancreatic islets. **(D)** Overlap of the significantly up-regulated or down-regulated genes in β-PPARα and β-HNF4α pancreatic islets. **(E)** The major GO pathways and GO pathways highly affected by β-PPARα and β-HNF4α overexpression in each group. The numbers in the brackets describe fold-enrichment and FDR, respectively. **(F)** The list of genes that was significantly up-regulated in adiponectin KO islets but down-regulated in β-PPARα and β-HNF4α pancreatic islets. **(G)** The list of genes that was significantly down-regulated in adiponectin KO islets but up-regulated in β-PPARα and β-HNF4α pancreatic islets. **(H)** Representative image of immunofluorescence of the adiponectin KO pancreas. IAPP (red), Insulin (green) and DAPI (blue). Scale bar indicates 100 μm. **(I)** The calculation of the average signal intensity of IAPP immunofluorescence. (n = 8–10) **(J)** The schematic representation of potential adiponectin action cascade on the pancreatic islets through HNF4α and PPARα. Data are mean ± SEM. $^{**}P < 0.01$ and $^{****}P < 0.0001$. Unpaired 2-tailed t-tests were utilized for determining the p-values for **(A)** and **(I)**.

capacity of the islets. Also, islets isolated from PPARα KO mice show higher basal insulin secretion but impaired GSIS [26], suggesting that lowered fatty acid oxidation deteriorates GSIS, because PPARα in the islet is the major determinant of islet fatty acid oxidation [27]. On the other hand, our data suggest that the overexpression of PPARα in pancreatic β cells *in vivo* decreases insulin secretion despite improved lipotoxicity including lower dihydroceramides and ceramides. Consistent with these observations, excessive fatty acid oxidation by overexpression of PPARα in the INS β cells lowers insulin secretion [28]. LRP1 KO mice and β cell-specific PPARγ overexpression mice phenocopy β-PPARα overexpression, as judged by decreased islet ceramide levels and lower insulin secretion [29].

In addition, we discovered that two major phospholipids, PE and PC, were significantly reduced in β-PPARα islets. Phospholipase A2, the enzyme that catalyzes the conversion of phospholipids to lysophospholipids and arachidonic acids, enhances insulin secretion through its metabolites by inhibiting K_{ATP} channel [30,31]. Essential phospholipids also protect from islet damage and prevent inflammation [32]. This might be related to the fact that the serum PC levels are down-regulated in overt type 1 diabetic and type 2 diabetic patients [33,34]. These data raise the possibility that the reduced insulin secretion by β-PPARα overexpression may not only be caused by lowered ceramides, but also, at least in part, by the lowered islet phospholipids. While the enhanced fatty acid oxidation by PPARα can be beneficial for the reduction of ceramide species, the decline of phospholipids might have deleterious effects on insulin secretion.

We previously reported that adiponectin overexpression increased the regenerative capacity after the caspase-8-mediated apoptosis [9]. Adiponectin receptor (AdipoR) preserves the function of pancreatic β cells through the AMPK signaling pathway. AMPK activates the major transcription factors for β cell differentiation, Pdx-1 through PPARα [35]. Therefore, we assumed that the downstream targets of adiponectin, including PPARα, can induce islet expansion.

However, β-PPARα overexpression uniformly down-regulated insulin production and had little impact on the expansion of pancreatic β cells or differentiation to other types of endocrine cells. Our data suggests that PPARα in pancreatic β cells is beneficial to up-regulate fatty acid oxidation, but does not seem to be involved in the proliferation of pancreatic β cells. Given that adiponectin receptor agonist chronically enhances AdipoR signaling [12], thus preserving β cells, β-PPARα overexpression might be more beneficial for *preserving* pancreatic β cells under glucolipotoxic conditions rather than enhancing *proliferation* of pancreatic β cells.

Constitutive deletion of HNF4α by insulin promotor-driven *Cre* results in the impairment of the physiological expansion of β cells during pregnancy and GSIS [36,37]. In line with this, genetic mutations of HNF4α that are known as MODY1 manifest as an autosomal dominant form of type 2 diabetes and is characterized by neonatal hypoglycemia and the defect of GSIS [38]. HNF4α regulates genes that are involved in the cholesterol, fatty acid, amino acid and glucose metabolism [39]. In contrast to the beneficial functions of HNF4α on β cell differentiation during developmental stages, in vitro studies demonstrate that HNF4α in adult islets suppresses the expansion of the islets by dysregulation of DNA synthesis and loss of β cell lineage [40]. Also, an HNF4α antagonist enhances the β cell replication in adult mice [41]. Our study demonstrates the consequences of β cell-specific, doxycycline inducible overexpression of HNF4α during the adult stage, which triggers hyperglycemia and the loss of β cell expansion that is normally driven by HFD. These findings corroborate the previous findings of HNF4α on the cellular physiology of the β cell in the adult stage, and very much contrast with the function of HNF4α during development. Considering the deleterious impact of HNF4α on β cell replication *in vivo*, HNF4α expression can be counter-regulated and reduced to make up for the impaired insulin secretion in the adiponectin KO mice. Both HNF4α and PPARα are involved in fatty acid oxidation [20]. However, the relationship of these transcription factors to each other has not been elucidated. We discovered that HNF4α overexpression dramatically induces PPARα expression but not *vice versa*, placing HNF4α up-stream of PPARα. Analysis of the overlap of the genes significantly affected by overexpression of HNF4α and PPARα reveals that fatty acid oxidation is up-regulated and insulin secretion is down-regulated. Although there are substantial overlaps of genes between HNF4α and PPARα, we could also find gene pathways independently regulated, such as ribosomal small subunit assembly by PPARα and endocrine pancreas development by HNF4α.

By combining the RNA-seq data from adiponectin KO, β- PPARα and β-HNF4α, we found a very important role for IAPP that is regulated consistent with a model outlining an adiponectin-HNF4α-PPARα cascade. IAPP, also known as amylin, is a hormone secreted from β cells. Since the levels of IAPP go hand in hand with the levels of C-peptide [42], serum IAPP levels reflect β cell function. However, it is also known that IAPP aggregates in diabetic β cells and negatively affects insulin secretion [43,44]. IAPP fibril formation and elongation are enhanced on phospholipid bilayers [31]. Moreover, negatively charged phospholipids accelerate the aggregation of human IAPP [45], consistent with the fact that lower PC levels and the lower IAPP levels are seen in β-PPARα islets. Human IAPP is considerably more amyloidogenic and causes cytotoxicity compared to rodent IAPP [46]. Nonetheless, given that IAPP deficient mice show increased insulin responses [47], an increase of IAPP in adiponectin KO mice can unquestionably exert a negative effect on insulin secretion. IAPP is also known to induce apoptosis through ceramide synthesis [48]. Adiponectin deficiency induces ceramide accumulation, that could be mediated through IAPP, particularly in islets.

We determined a cascade of adiponectin-HNF4α-PPARα in pancreatic β cells. The latter two of these factors are known to regulate fatty acid oxidation and cholesterol metabolism [20]. The genes are regulated in a similar fashion by both HNF4α and PPARα which explains the common phenotype of β-PPARα and β-HNF4α mice, and *vice versa*. Importantly, our studies here highlight just one downstream pathway of adiponectin in β cells, and they do not capture the whole impact of adiponectin on islets. Notably, even though HNF4α and PPARα are consistently regulated in islets of adiponectin KO and adiponectin overexpressing mice, the insulin secretion phenotype is inconsistent between adiponectin KO mice and β-PPARα and β-HNF4α mice. One possibility is that adiponectin regulates another molecule that modulates the negative impact of PPARα and HNF4α on insulin secretion. Another possibility is that PPARα and HNF4α might be down-regulated in adiponectin KO mice as a compensatory mechanism to maintain the insulin secretory capacity.

Collectively, our data demonstrates adiponectin, PPARα and HNF4α function in concert in pancreatic β cells. Our study paves the way for a better understanding of the important adiponectin biology and its downstream targets in the islets. Further appreciation of the molecular basis of lipid metabolism and insulin secretion in pancreatic islets is still required for the development of better clinical interventions. Adiponectin unquestionably is a critical mediator of islet functionality.

AUTHOR CONTRIBUTIONS

T.O. and D.-S.K. designed and performed the experiments and contributed equally. T.O and D.-S.K. acquired data with the help of R.Y., M.Y.W., L.S., B.F., C.Li., X.S. and P.E.S. T.O. and P.E.S. interpreted the data and wrote the manuscript. C.M.K. provided experimental guidance and helped the manuscript preparation. S.C. was in charge of surgery and islet perfusion. M.P. and C.L. assisted in histology. R.G. assisted in sphingolipid analysis. C.C. and S.Z. provided the feedback on the manuscript. P.E.S. is the guarantor of this work and, as such, had full access to all the data in the study and takes

responsibility for the integrity of the data and the accuracy of the analysis.

DECLARATION OF COMPETING INTEREST

The authors declare that they have no known competing financial interests or personal relationships that could have appeared to influence the work reported in this paper.

DATA AVAILABILITY

Data will be made available on request.

ACKNOWLEDGMENTS

We thank the UTSW Animal Resource Center, Histology Core, Metabolic Phenotyping Core, Transgenic Core for their excellent assistance with experiments performed here. We thank Shimadzu Scientific Instruments and Shimadzu Corporation for the collaborative efforts in mass spectrometry technology resources. This study was supported by US NIH grants RC2-DK118620, R01-DK55758, R01-DK099110, R01-DK127274 and R01-DK131537 to P.E.S. S.Z. was supported by a US National Institutes of Health grant R00-AG068239 and a Voelcker Fund Young Investigator Pilot grant. C.C. was supported by US NIH grant R00-DK122019. Research reported in this publication was also supported by the UTSWNORC grant under US NIDDK/NIH award number P30-DK127984.

APPENDIX A. SUPPLEMENTARY DATA

Supplementary data to this article can be found online at https://doi.org/10.1016/j.molmet.2023.101821.

REFERENCES

[1] Poitout V, Robertson RP. Minireview: secondary beta-cell failure in type 2 diabetes–a convergence of glucotoxicity and lipotoxicity. Endocrinology 2002;143(2):339—42.
[2] Poitout V, Amyot J, Semache M, Zarrouki B, Hagman D, Fontes G. Glucolipotoxicity of the pancreatic beta cell. Biochim Biophys Acta 2010;1801(3):289—98.
[3] Wang H, Kouri G, Wollheim CB. ER stress and SREBP-1 activation are implicated in beta-cell glucolipotoxicity. J Cell Sci 2005;118(Pt 17):3905—15.
[4] Shimabukuro M, Zhou YT, Levi M, Unger RH. Fatty acid-induced beta cell apoptosis: a link between obesity and diabetes. Proc Natl Acad Sci U S A 1998;95(5):2498—502.
[5] Busch AK, Cordery D, Denyer GS, Biden TJ. Expression profiling of palmitate- and oleate-regulated genes provides novel insights into the effects of chronic lipid exposure on pancreatic beta-cell function. Diabetes 2002;51(4):977—87.
[6] Bacha F, Saad R, Gungor N, Arslanian SA. Adiponectin in youth: relationship to visceral adiposity, insulin sensitivity, and beta-cell function. Diabetes Care 2004;27(2):547—52.
[7] Okamoto M, Ohara-Imaizumi M, Kubota N, Hashimoto S, Eto K, Kanno T, et al. Adiponectin induces insulin secretion in vitro and in vivo at a low glucose concentration. Diabetologia 2008;51(5):827—35.
[8] Patane G, Caporarello N, Marchetti P, Parrino C, Sudano D, Marselli L, et al. Adiponectin increases glucose-induced insulin secretion through the activation of lipid oxidation. Acta Diabetol 2013;50(6):851—7.
[9] Ye R, Holland WL, Gordillo R, Wang M, Wang QA, Shao M, et al. Adiponectin is essential for lipid homeostasis and survival under insulin deficiency and promotes beta-cell regeneration. Elife 2014;3.
[10] Ye R, Wang M, Wang QA, Scherer PE. Adiponectin-mediated antilipotoxic effects in regenerating pancreatic islets. Endocrinology 2015;156(6):2019—28.
[11] Brown JE, Conner AC, Digby JE, Ward KL, Ramanjaneya M, Randeva HS, et al. Regulation of beta-cell viability and gene expression by distinct agonist fragments of adiponectin. Peptides 2010;31(5):944—9.
[12] Onodera T, Ghazvini Zadeh E, Xu P, Gordillo R, Guo Z, Joffin N, et al. PEGylated AdipoRon derivatives improve glucose and lipid metabolism under insulinopenic and high-fat diet conditions. J Lipid Res 2021;62:100095.
[13] Esmaili S, Xu A, George J. The multifaceted and controversial immunometabolic actions of adiponectin. Trends Endocrinol Metabol 2014;25(9):444—51.
[14] Ye R, Wang M, Wang QA, Spurgin SB, Wang ZV, Sun K, et al. Autonomous interconversion between adult pancreatic α-cells and β-cells after differential metabolic challenges. Mol Metabol 2016;5(7):437—48.
[15] Kusminski CM, Chen S, Ye R, Sun K, Wang QA, Spurgin SB, et al. MitoNEET-parkin effects in pancreatic alpha- and beta-cells, cellular survival, and intrainsular cross talk. Diabetes 2016;65(6):1534—55.
[16] Zhang Z, Funcke JB, Zi Z, Zhao S, Straub LG, Zhu Y, et al. Adipocyte iron levels impinge on a fat-gut crosstalk to regulate intestinal lipid absorption and mediate protection from obesity. Cell Metabol 2021;33(8):1624—1639 e1629.
[17] Partridge L, Gems D, Withers DJ. Sex and death: what is the connection? Cell 2005;120(4):461—72.
[18] Li Z, Agellon LB, Allen TM, Umeda M, Jewell L, Mason A, et al. The ratio of phosphatidylcholine to phosphatidylethanolamine influences membrane integrity and steatohepatitis. Cell Metabol 2006;3(5):321—31.
[19] Puri P, Baillie RA, Wiest MM, Mirshahi F, Choudhury J, Cheung O, et al. A lipidomic analysis of nonalcoholic fatty liver disease. Hepatology 2007;46(4):1081—90.
[20] Chamouton J, Latruffe N. PPARalpha/HNF4alpha interplay on diversified responsive elements. Relevance in the regulation of liver peroxisomal fatty acid catabolism. Curr Drug Metabol 2012;13(10):1436—53.
[21] Hull RL, Westermark GT, Westermark P, Kahn SE. Islet amyloid: a critical entity in the pathogenesis of type 2 diabetes. J Clin Endocrinol Metab 2004;89(8):3629—43.
[22] Mao X, Kikani CK, Riojas RA, Langlais P, Wang L, Ramos FJ, et al. APPL1 binds to adiponectin receptors and mediates adiponectin signalling and function. Nat Cell Biol 2006;8(5):516—23.
[23] Wang C, Li X, Mu K, Li L, Wang S, Zhu Y, et al. Deficiency of APPL1 in mice impairs glucose-stimulated insulin secretion through inhibition of pancreatic beta cell mitochondrial function. Diabetologia 2013;56(9):1999—2009.
[24] Holland WL, Miller RA, Wang ZV, Sun K, Barth BM, Bui HH, et al. Receptor-mediated activation of ceramidase activity initiates the pleiotropic actions of adiponectin. Nat Med 2011;17(1):55—63.
[25] Li N, Zhao S, Zhang Z, Zhu Y, Gliniak CM, Vishvanath L, et al. Adiponectin preserves metabolic fitness during aging. Elife 2021;10.
[26] Bihan H, Rouault C, Reach G, Poitout V, Staels B, Guerre-Millo M. Pancreatic islet response to hyperglycemia is dependent on peroxisome proliferator-activated receptor alpha (PPARalpha). FEBS Lett 2005;579(11):2284—8.
[27] Yoshikawa H, Tajiri Y, Sako Y, Hashimoto T, Umeda F, Nawata H. Effects of free fatty acids on beta-cell functions: a possible involvement of peroxisome proliferator-activated receptors alpha or pancreatic/duodenal homeobox. Metabolism 2001;50(5):613—8.
[28] Tordjman K, Standley KN, Bernal-Mizrachi C, Leone TC, Coleman T, Kelly DP, et al. PPARalpha suppresses insulin secretion and induces UCP2 in insulinoma cells. J Lipid Res 2002;43(6):936—43.
[29] Ye R, Gordillo R, Shao M, Onodera T, Chen Z, Chen S, et al. Intracellular lipid metabolism impairs beta cell compensation during diet-induced obesity. J Clin Invest 2018;128(3):1178—89.
[30] Bao S, Jacobson DA, Wohltmann M, Bohrer A, Jin W, Philipson LH, et al. Glucose homeostasis, insulin secretion, and islet phospholipids in mice that overexpress iPLA2beta in pancreatic beta-cells and in iPLA2beta-null mice. Am J Physiol Endocrinol Metab 2008;294(2):E217—29.

[31] Knight JD, Miranker AD. Phospholipid catalysis of diabetic amyloid assembly. J Mol Biol 2004;341(5):1175—87.
[32] Shahbazov R, Kanak MA, Takita M, Kunnathodi F, Khan O, Borenstein N, et al. Essential phospholipids prevent islet damage induced by proinflammatory cytokines and hypoxic conditions. Diabetes Metab Res Rev 2016;32(3):268—77.
[33] Lamichhane S, Ahonen L, Dyrlund TS, Kemppainen E, Siljander H, Hyoty H, et al. Dynamics of plasma lipidome in progression to islet autoimmunity and type 1 diabetes - type 1 diabetes prediction and prevention study (DIPP). Sci Rep 2018;8(1):10635.
[34] Wigger L, Barovic M, Brunner AD, Marzetta F, Schoniger E, Mehl F, et al. Multi-omics profiling of living human pancreatic islet donors reveals heterogeneous beta cell trajectories towards type 2 diabetes. Nat Metab 2021;3(7):1017—31.
[35] Guo H, Sun S, Zhang X, Zhang XJ, Gao L, Zhao JJ. AMPK enhances the expression of pancreatic duodenal homeobox-1 via PPARalpha, but not PPARgamma, in rat insulinoma cell line INS-1. Acta Pharmacol Sin 2010;31(8):963—9.
[36] Gupta RK, Vatamaniuk MZ, Lee CS, Flaschen RC, Fulmer JT, Matschinsky FM, et al. The MODY1 gene HNF-4alpha regulates selected genes involved in insulin secretion. J Clin Invest 2005;115(4):1006—15.
[37] Gupta RK, Gao N, Gorski RK, White P, Hardy OT, Rafiq K, et al. Expansion of adult beta-cell mass in response to increased metabolic demand is dependent on HNF-4alpha. Genes Dev 2007;21(7):756—69.
[38] Byrne MM, Sturis J, Fajans SS, Ortiz FJ, Stoltz A, Stoffel M, et al. Altered insulin secretory responses to glucose in subjects with a mutation in the MODY1 gene on chromosome 20. Diabetes 1995;44(6):699—704.
[39] Chen L, Luo S, Dupre A, Vasoya RP, Parthasarathy A, Aita R, et al. The nuclear receptor HNF4 drives a brush border gene program conserved across murine intestine, kidney, and embryonic yolk sac. Nat Commun 2021;12(1):2886.
[40] Rieck S, Zhang J, Li Z, Liu C, Naji A, Takane KK, et al. Overexpression of hepatocyte nuclear factor-4alpha initiates cell cycle entry, but is not sufficient to promote beta-cell expansion in human islets. Mol Endocrinol 2012;26(9):1590—602.
[41] Lee SH, Piran R, Keinan E, Pinkerton A, Levine F. Induction of beta-cell replication by a synthetic HNF4alpha antagonist. Stem Cell 2013;31(11):2396—407.
[42] Hartter E, Svoboda T, Ludvik B, Schuller M, Lell B, Kuenburg E, et al. Basal and stimulated plasma levels of pancreatic amylin indicate its co-secretion with insulin in humans. Diabetologia 1991;34(1):52—4.
[43] Rivera JF, Costes S, Gurlo T, Glabe CG, Butler PC. Autophagy defends pancreatic beta cells from human islet amyloid polypeptide-induced toxicity. J Clin Invest 2014;124(8):3489—500.
[44] Hernandez MG, Aguilar AG, Burillo J, Oca RG, Manca MA, Novials A, et al. Pancreatic beta cells overexpressing hIAPP impaired mitophagy and unbalanced mitochondrial dynamics. Cell Death Dis 2018;9(5):481.
[45] Jayasinghe SA, Langen R. Lipid membranes modulate the structure of islet amyloid polypeptide. Biochemistry 2005;44(36):12113—9.
[46] Westermark GT, Gebre-Medhin S, Steiner DF, Westermark P. Islet amyloid development in a mouse strain lacking endogenous islet amyloid polypeptide (IAPP) but expressing human IAPP. Mol Med 2000;6(12):998—1007.
[47] Gebre-Medhin S, Mulder H, Pekny M, Westermark G, Tornell J, Westermark P, et al. Increased insulin secretion and glucose tolerance in mice lacking islet amyloid polypeptide (amylin). Biochem Biophys Res Commun 1998;250(2):271—7.
[48] Zhang Y, Ranta F, Tang C, Shumilina E, Mahmud H, Foller M, et al. Sphingomyelinase dependent apoptosis following treatment of pancreatic beta-cells with amyloid peptides Abeta(1-42) or IAPP. Apoptosis 2009;14(7):878—89.

